Implementing and running CO model in g-CTMQC code using OpenMOLCAS for electronic structure calculations

Introduction

My project involved running electronic structure calculations in OpenMOLCAS to find Potential Energy Curves (PECs) for singlet carbon monoxide for a variety of CO bond lengths along with Non-Adiabatic Couplings (NACs). The results of these calculations were then implemented into the g-CTMQC code for dynamics calculations. However, the main goal of the project was not necessarily to learn anything about CO, rather, the goal was to gain experience with new electronic structure and dynamics software.

Overall, my current research interests are in exploring Nuclear Quantum Effects (NQEs), and towards the end we will likely be developing our own methods or codes for running dynamics with NQEs. As a result, I will need some experience with other codes to provide comparisons and benchmarks. Furthermore, we are interested in exact factorization methods, thus the g-CTMQC code which implements this is of particular interest. Therefore, while CO is chosen as the model, the overall goal is to grow comfortable with utilizing these methods for future comparisons with the methods we develop.

Finally, the use of the g-CTMQC code for my own molecule that is not currently implemented in the package is that the code currently does not have and interface with electronic structure software. Therefore, it provides another opportunity for me to learn other software from this workshop and hands-on experience with parameterizing adiabatic and diabatic states and programming them into the g-CTMQC package. As mentioned, previously, the OpenMOLCAS package will be utilized for the electronic structure calculations, and the resulting surfaces will then be coded into the g-CTMQC code providing me with some useful experience in both packages.

Methods

The electronic structure calculations were carried out in OpenMOLCAS using CASSCF and the CASPT2 level of theory. The ANO-R3 basis set was used and the active space was chosen to be (10,11) (electrons,orbitals). This is similar to active spaces common in literature for CO (usually the full valence (10,8))[1] with a few extra virtual orbitals that come close in energy to the HOMO-LUMO gap at large CO bond lengths. The NACs were computed near the coupling region the range of 2.0-2.3 Å.

The results from the electronic structure calculations were plotted and fitted in Maple 2019. For the adiabatic surfaces, generic morse potential functions were used and a linear fit was performed on the NACs. Using the NACs, the overlap angle in the adiabatic to diabatic transformation matrix was calculated according to:

$$\nabla\alpha = -F_{12} \quad (1)$$

where alpha is the mixing angle and F_{12} is the NAC as a function of nuclear coordinate R(which is CO bond length for this problem). In the 1-Dimensional case, this is easy to solve for alpha analytically and gives us alpha for the transformation matrix:

$$\boldsymbol{S} = \begin{bmatrix} \cos(2\alpha) & \sin(2\alpha) \\ -\sin(2\alpha) & \cos(2\alpha) \end{bmatrix} (2)$$

finally, we use the matrix **S** in Eq. 2 to convert the adiabatic potential to the diabatic potential and find our diabatic PECs using:

$$\mathbf{U}=\mathbf{S}^{T}\mathbf{V}\mathbf{S} \ (3)$$

where **U** is our diabatic potential energy matrix and **V** is our adiabatic potential energy matrix.[2] This provides us with the diabatic PECs and couplings that are needed for g-CTMQC.

Another method was also utilized to attempt to properly compute and parameterize the diabatic surfaces and couplings. In this computation, the diabatic surfaces were first found by following the state character which is reported from the CASSCF calculations. These surfaces were parametrized and the following equation was used to find the diabatic coupling[3]:

$$E_{\pm} = \frac{V11+V22}{2} \pm \frac{\sqrt{(V11-V22)^2+4V12^2}}{2} \ (4)$$

where VXY are the diabatic potential matrix elements, E_+ is the 1st excited adiabatic state and E_- is the ground adiabatic state. Using this equation, the diabetic coupling was optimized to provide the correct transformation from the diabatic states to the known adiabatic states.

Finally, after the diabatic matrix elements were properly computed and added to the g-CTMQC code, dynamics simulations were carried out. At first, the collision of carbon and oxygen and CO. The starting position of the wave packet was 7 bohr compared to the equilibrium bond distance of 2.1322 bohr with an initial momentum of -16 1/bohr. CT-MQC, TSHFS, and Ehrenfest dynamics calculations were carried out with the g-CTMQC code. These dynamics were performed on the surfaces computed with Eq. 3, however, it was found the NACs were incorrect. The surfaces from Eq. 4 simulated photodissociation of CO, with the wavepacket starting at a bond distance of 2.55 bohr (the bottom of the excited states well), with no initial momentum and a sigma of 0.08 a.u. using CT-MQC and TSHFS.

Results

The ground states energies of the equilibrium geometry at the CASPT2 level of theory were -113.212 Hartrees which agreed well with literature values of -113.13579 Hartrees. Furthermore, the SCF orbitals aligned with the general MO picture of the CO molecule. Based on this comparison, it was assumed that the method and active space would provide the necessary accuracy for this project and there were no significant errors. Furthermore, the PECs followed the expected Morse potential for the dissociation of a diatomic, which was also found in the literature. The adiabatic PECs of the ground and first excited state of CO are given in Figure 1. Notice that for points at longer distances, there is some discontinuity in the behavior of the tail. It should approach an asymptote, however, there are steps at certain points. Upon

investigation, it was found that the CASPT2 calculation resulted in significant changes in the weights and coefficients of configurations which is a sign of intruder states and erroneous calculations. The energies were recalculated with an imaginary shift of 0.1 and 0.2 to attempt to resolve this but to no avail. Unfortunately due to time constraints, I opted to remove these points from the final data set as the energies were not correct, the corrected PECs are given in Figure 2.

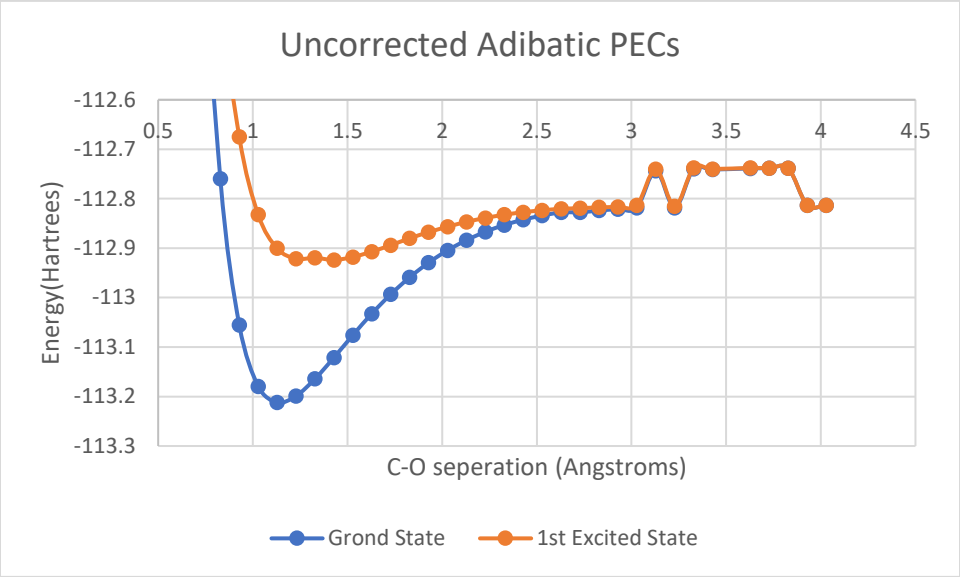

Figure 1. The adiabatic PECs of CO with the erroneous points at the tail.

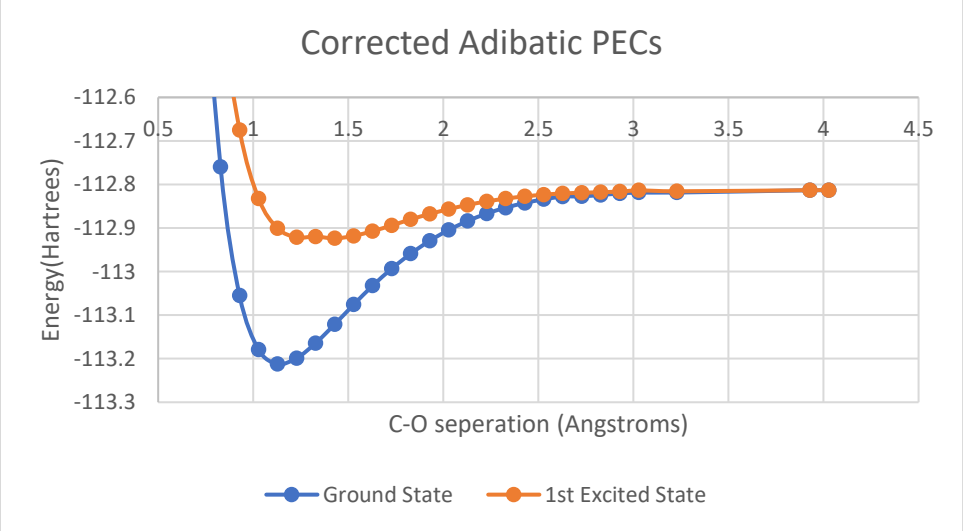

Figure 2. The adiabatic PECs of CO with the erroneous points removed from the tail.

The PECs were imported to Maple 2019 where the curve fitting was performed. The results of each fit are given in Figures 3 and 4 along with the equation.

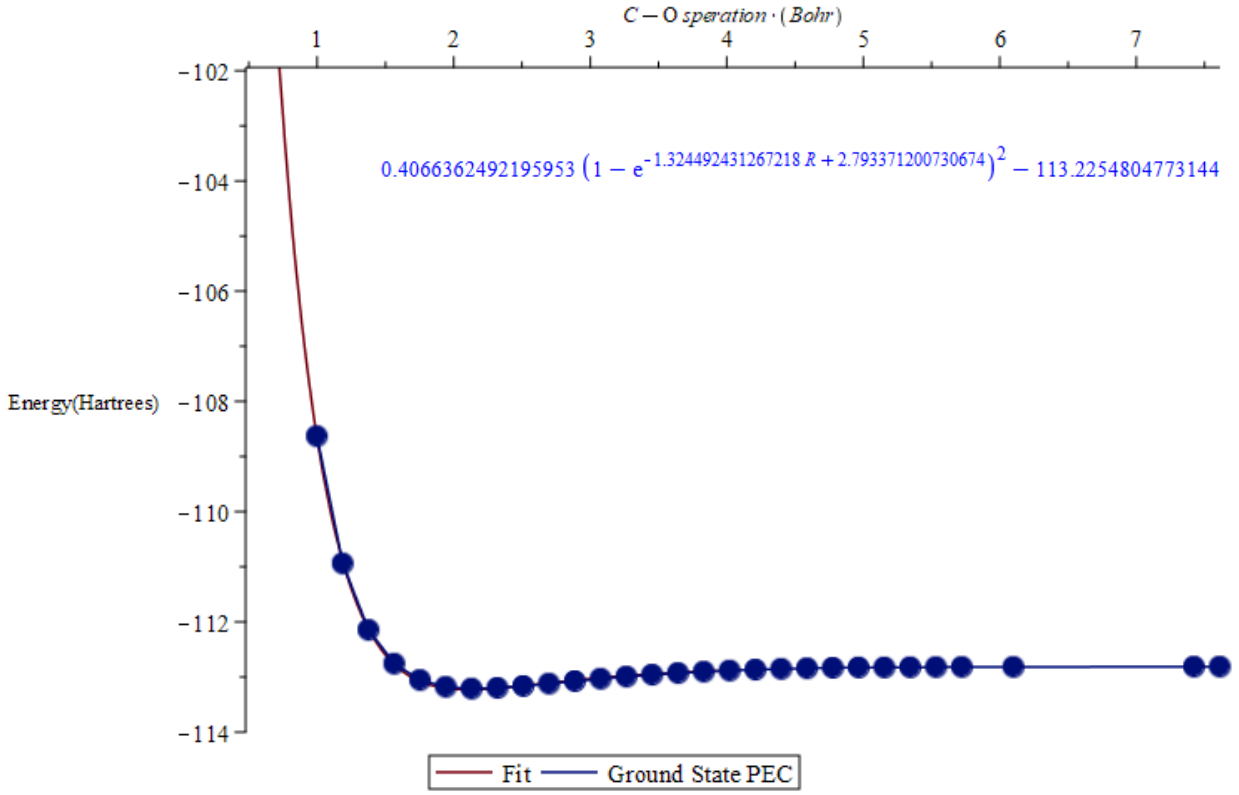

Figure 3: Ground state PEC with fitting function and curve.

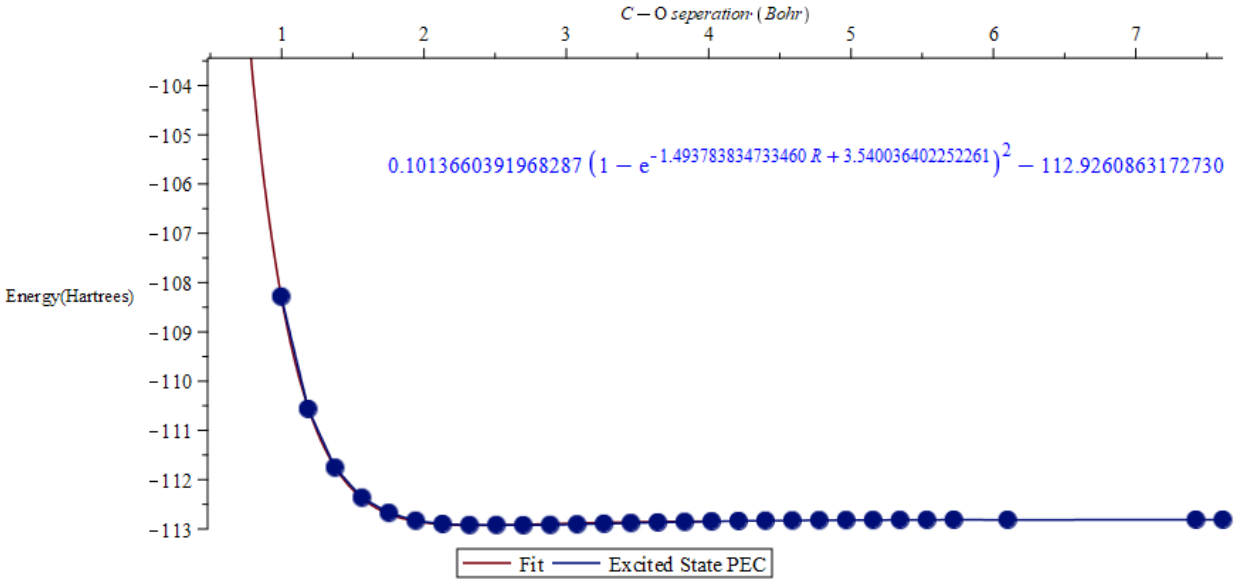

Figure 4: Excited state PEC with fitting function and curve.

Additionally, the NACs and their fit are given below in Figure 5.

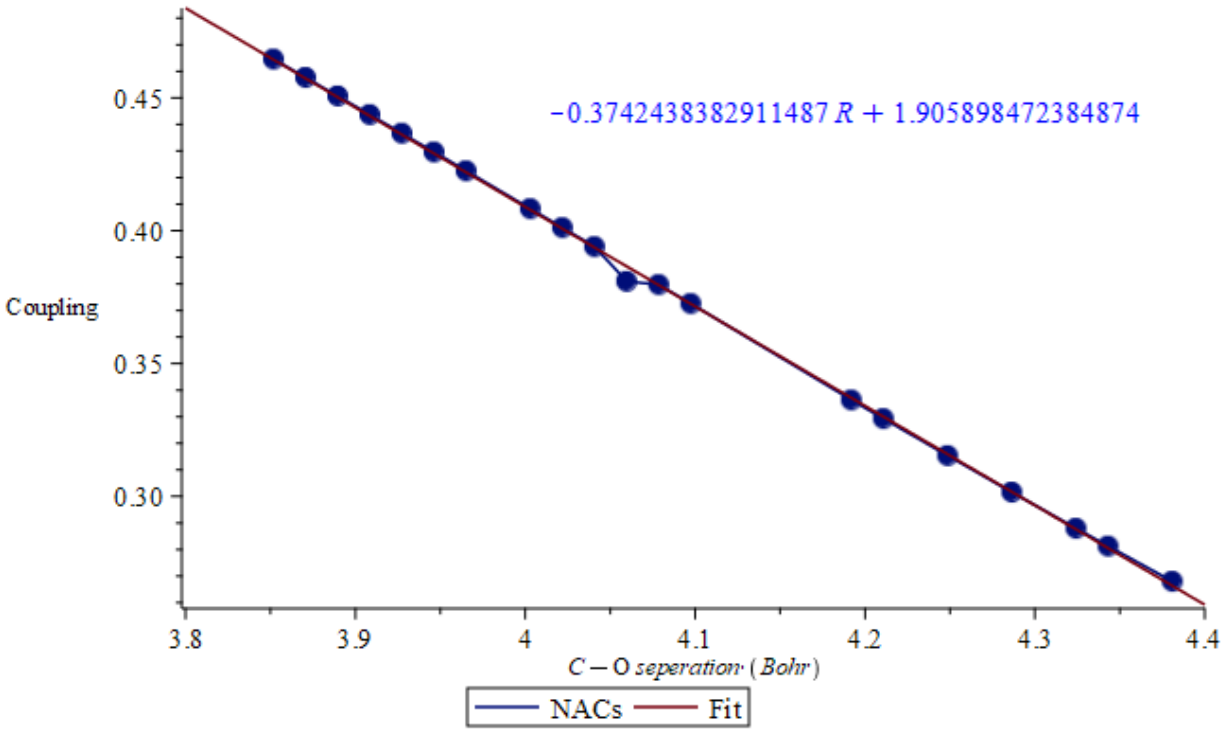

Figure 5. NACs in the range of 2.0-2.3 angstroms along with the fit and function.

The NACs given in Figure 5 appear to continuously grow, however, they are much smaller near the equilibrium distance which was not probed here. It is likely that the sampled range was not large enough and a range needed to be sampled but this was not possible due to time constraints. It should also be mentioned that at first it was assumed that the adiabatic surfaces themselves could be added to the g-CTMQC code without any coupling as that would be calculated by the software. However, it was found that the diabatic states and their couplings were necessary for coupling to be computed at all, as a result, the NACs and the diabatic states were computed much later in the project with far less time to optimize the process. Using these functions and the transformation given in the Methods section, the diabatic states were computed analytically. The functions themselves were quite messy, and so only plots of the diabatic states and coupling are given in Figures 6 and 7 respectively.

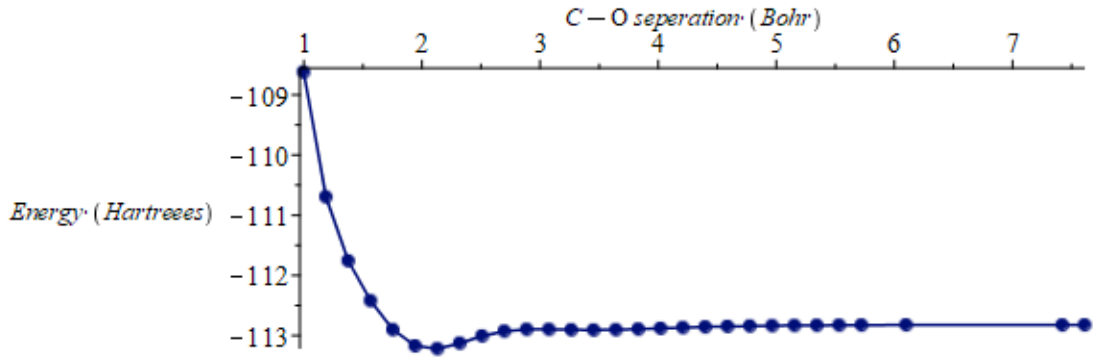

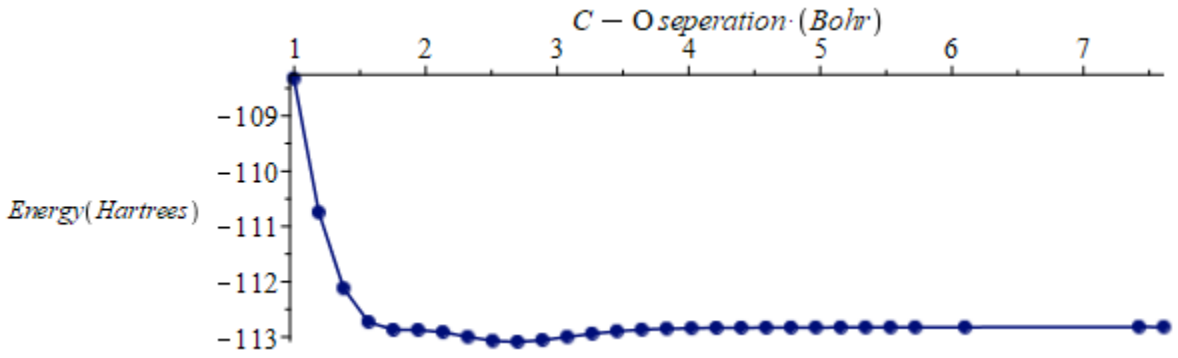

Figure 6. Diabatic ground(top) and excited(bottom) states computed from the transformation.

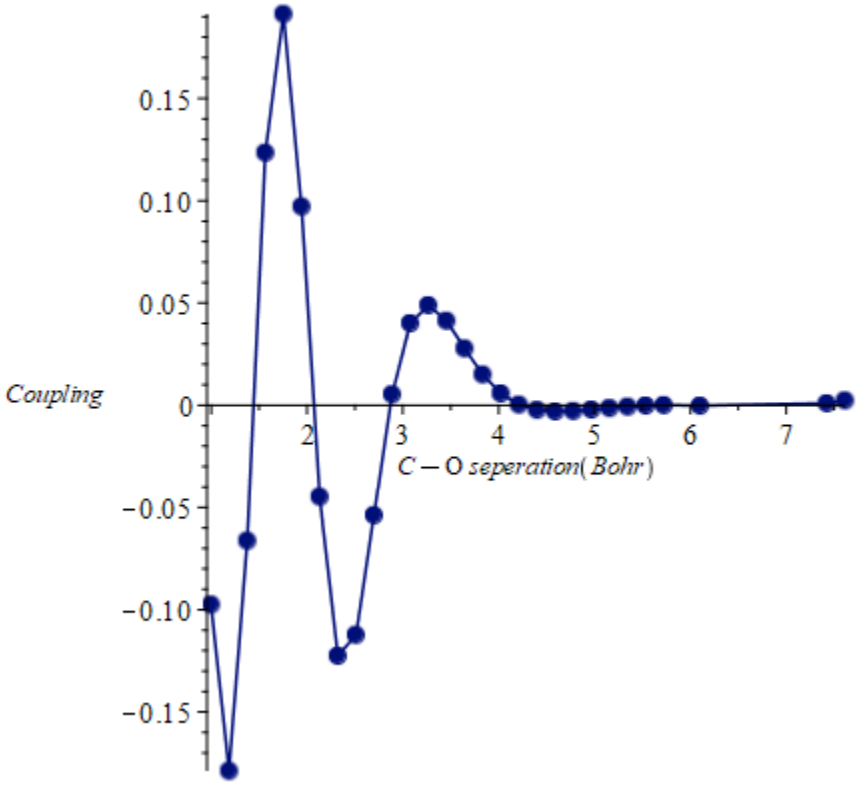

Figure 7. Diabatic coupling computed from the transformation. The behavior towards the smaller internuclear distances may be an artifact of the transformation or NACs as they were not run for the largest range.

Finally, the diabatic surfaces and couplings given above were added to the g-CTMQC code and dynamics could be run. However, these results are not discussed in this report, as it was discovered that the NACs were computed incorrectly as the wrong data was used. As a result, another attempt at computing the proper diabatic surfaces and couplings using Eq. 4 was made. For this method, the diabatic surfaces were found by following the character of each state and the resulting diabatic surfaces for the ground state configuration and $\pi\pi^*$ transitions are given in Figure 8.

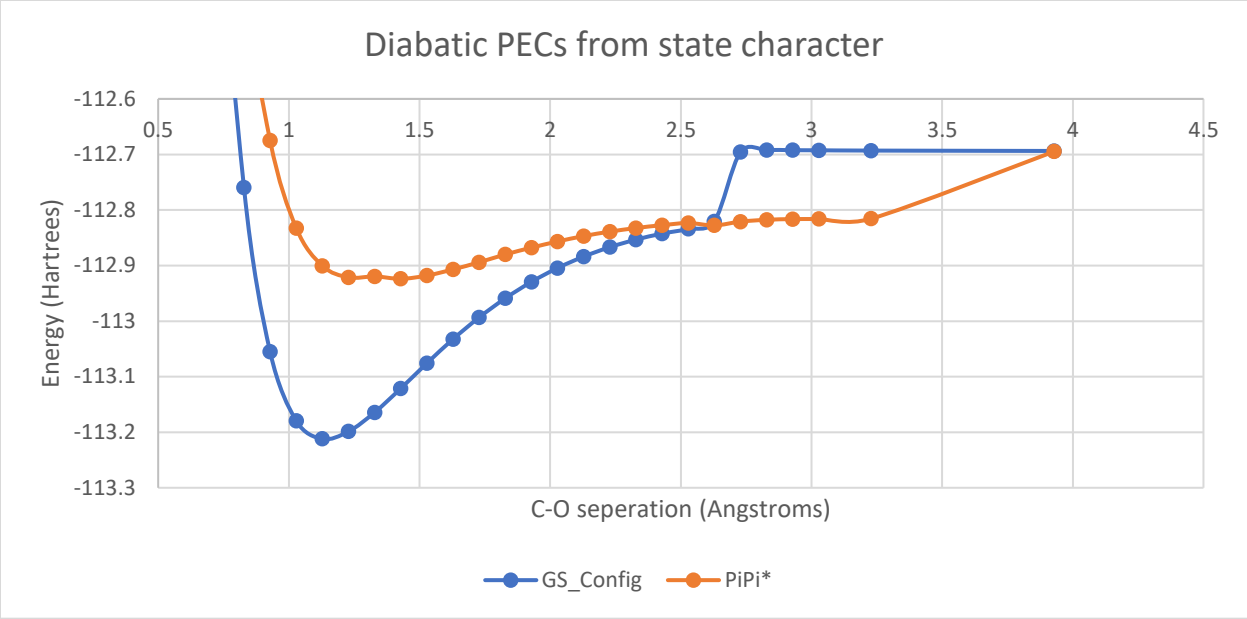

Figure 8. Diabatic states for ground state configuration and ππ* transitions

These surfaces were fit using maple just as the adiabatic surfaces. The fitting results and functions are given in Figure 9.

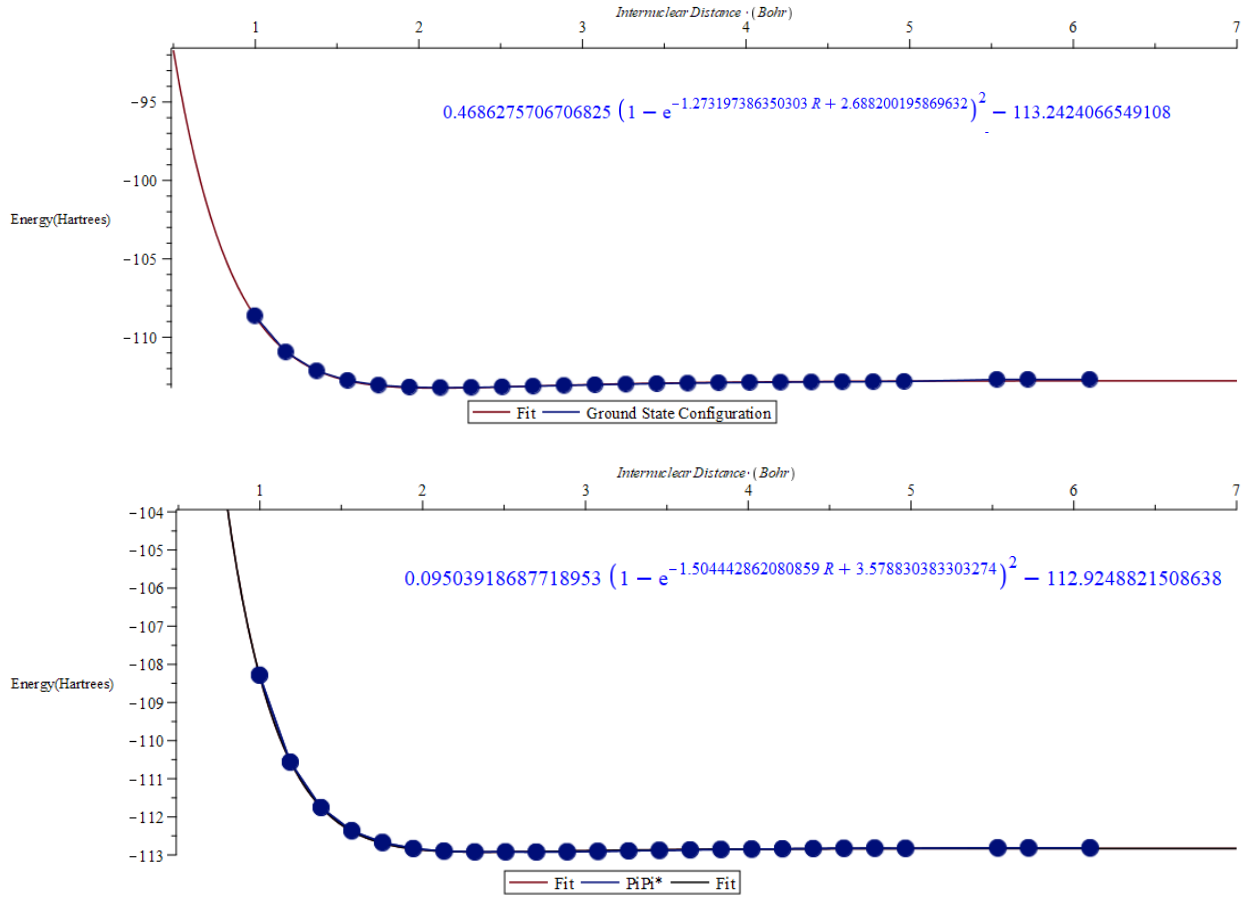

Figure 9. Diabatic states for ground state configuration and ππ* transitions and there curve fitting and functions

From Eq. 9, the couplings were calculated to be approximately gaussian and the parameters were optimized using Eq.4 and the transformation to the adiabatic states. The resulting coupling is given in Figure 10.

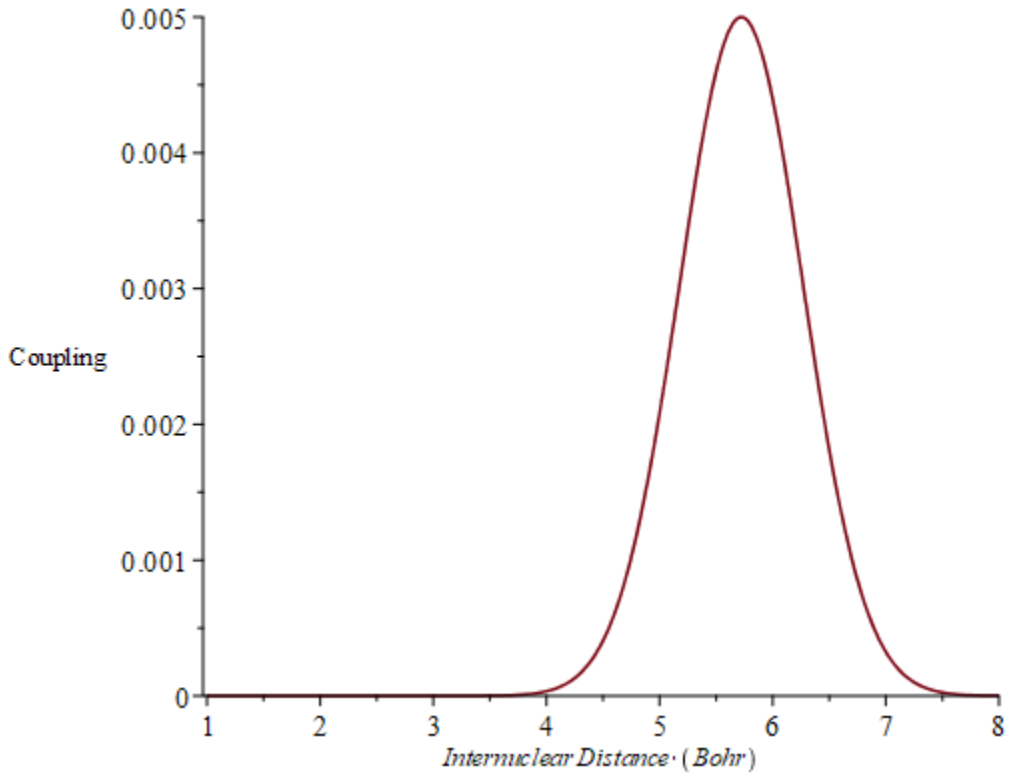

Figure 10. Diabatic coupling computed using Eq.4 and optimizing transformed diabetic states.

Unfortunately, the coupling was region was found to be at a large internuclear distance and there were not many CASSCF calculations performed in this region. As a result, the fitting is crude at best and due to time constraints, more CASSCF calculations could not be performed in time to provide better results. Thus, this crude coupling and the resulting adiabatic states were added to the CT-MQC code to perform at least some dynamics on the surface.

The results of the dynamics calculation are given below in Figure 11.

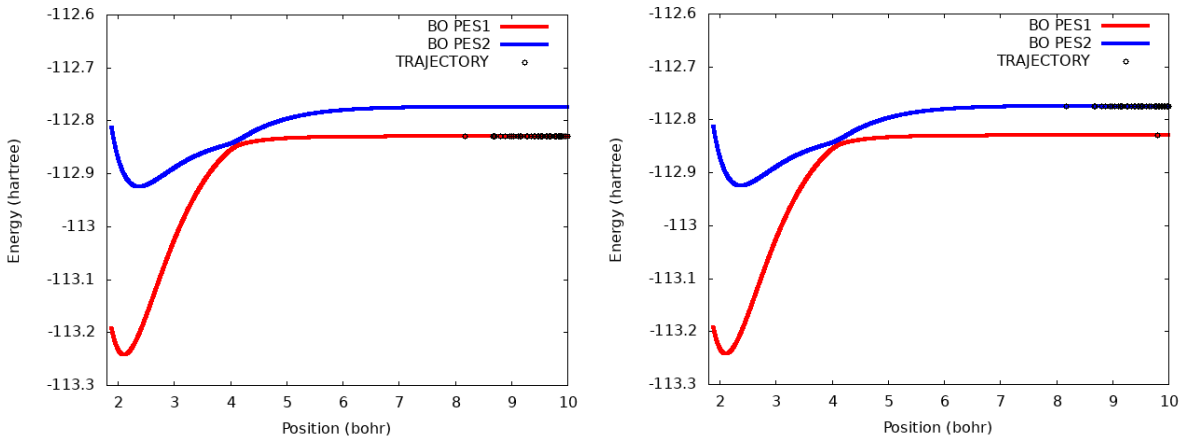

Figure 11. Trajectories on the adiabatic PECs of CO. CT-MQC result on the left and TSHFS on the right.

From above, the adiabatic states were relatively well reproduced from the diabatic transformation, especially before the coupling region. After the coupling region, the excited state increases somewhat in energy, it is only a few hundredths of a Hartrees off from the adiabatic surface which provides some indication to the error in the coupling term. With a better sampling of the coupling region, it may have been possible to improve these surfaces, however, this was not possible due to time constraints. Regardless, we can make some conclusions of the TSHFS methods and CT-MQC results. In the CT-MQC result, we see the entire wave packet move to the ground state shortly after the surfaces come near each other. The trajectories moving to the other surface after the surfaces come close is potentially an artifact of the poor diabatic coupling term. What is interesting, is that in the TSHFS method we only see surface hopping where the states come together. Furthermore, they appear to mostly remain on the excited state. Finally, the populations and coherence data are given below in Figure 12.

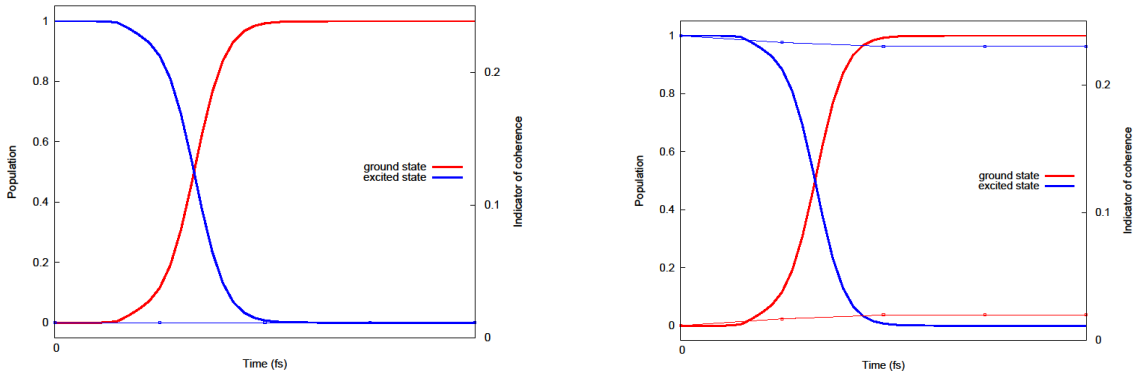

Figure 12. Populations and coherences for CT-MQC(Right) and TSHFS(Left) calculations

For both methods, the populations follow similar trends, however, the TSHFS method suffers from some issues with overcoherence in the excited state which are not encountered in the ground state.

Conclusion

Overall, it should be restated again that there were multiple parts of the analysis that could be improved. For one, the discovery of incorrect data in the NAC computation only facilitated issues with a lack of time to better parameterize the diabatic and adiabatic surfaces. This was particularly problematic for the second attempt at computing the diabatic states, as additional CASSCF calculations which were needed to better compute the coupling could not be performed. Additionally, the CT-MQC calculations themselves could be ran with more trajectories or for longer times. Regardless, due to time-constraints, these points are unable to be addressed, and a proper exploration of diabatic transformations, NACs and other initial conditions for the dynamics were unable to be explored in this project. However, the obtained results are still reasonable, despite the shortcomings of the methods. Finally, the overall goal of the project was not to obtain publishable results of dynamics on CO. The main objective was to use and gather experience with the g-CTMQC code and OpenMOLCAS, and parameterizing similar systems and to this end the project was successful.

References

1. Peterson, K. and Woods, R., 1990. Theoretical dipole moment functions involving the a 3Π and a’ 3Σ+ states of carbon monoxide. *J. Chem. Phys.*, 93(7), pp.5029-5036.
2. Köppel, H., 2004. DIABATIC REPRESENTATION: METHODS FOR THE CONSTRUCTION OF DIABATIC ELECTRONIC STATES. *Advanced Series in Physical Chemistry*, pp.175-204.
3. Izmaylov, A. and Franco, I., 2016. Entanglement in the Born–Oppenheimer Approximation. *J. Chem. Theory Comput.*, 13(1), pp.20-28.